Electronic Supplementary Information

of

Dual-standard matrix-matched calibration strategy for LA-ICP-MS elemental quantitative imaging of calcium oxalate-uric acid dual-matrix urinary stones

Xinyi Chen[a,b], Qingling Zhou[a,b], Duoduo Ao[a,b], Hui Hu[a,b], Hui Xu[c], Tengfei Zheng[a,b], Yongmei Hu[a], Ying Ye[a], Xiaoqing Yi[c], Jianzong Zhou[a,b,*], Yuqiu Ke[a,b,*]

[a] Key Laboratory of Testing and Tracing of Rare Earth Products, State Administration for Market Regulation, Jiangxi University of Science and Technology, Ganzhou 341000, P.R. China

[b] Jiangxi Provincial Key Laboratory of Functional Crystalline Materials Chemistry, Jiangxi University of Science and Technology, Ganzhou 341000, P.R. China

[c] Research Center of Jiangxi Province for Engineering Technology of Calculus Prevention and Control, Gannan Medical University, Ganzhou 341000, P.R. China

*Corresponding author:

Yuqiu Ke (keyuqiu@cug.edu.cn)

Key Laboratory of Testing and Tracing of Rare Earth Products, State Administration for Market Regulation, Jiangxi University of Science and Technology, Ganzhou 341000, P.R. China

Jianzong Zhou (zhoujianzong43@126.com)

Jiangxi Provincial Key Laboratory of Functional Crystalline Materials Chemistry, Jiangxi University of Science and Technology, Ganzhou 341000, P.R. China

Chemicals and materials

Ultrapure water (resistivity: 18.2 MΩ cm), obtained from a water purification system (Hitech Pure Water Technologies, China), was used throughout the study for the preparation of blanks, calibration standards, and solutions. Nitric acid (HNO_3, guaranteed reagent grade; Xilong Co. Ltd., China) was further purified by sub-boiling distillation to obtain high-purity HNO_3, which was subsequently used for sample digestion and solution preparation. A mixed standard solution (~500 μg g^{-1} per element, Solution A) was prepared by dissolving the following salts in 2 wt.% HNO_3 solution: $Mg(NO_3)_2 \cdot 6H_2O$ (1.0676 g), $Cr(NO_3)_3 \cdot 9H_2O$ (0.7658 g), $MnSO_4 \cdot H_2O$ (0.3604 g), $Co(NO_3)_2 \cdot 6H_2O$ (0.5006 g), $Cu(NO_3)_2 \cdot 3H_2O$ (0.3825 g), $Zn(NO_3)_2 \cdot 6H_2O$ (0.4627 g), $Sr(NO_3)_2$ (0.2447 g). All chemical reagents, including the above nitrates and sulfates, as well as uric acid (UA), sodium hydroxide (NaOH), and glacial acetic acid (≥99.5%), were of analytical reagent (AR) grade and purchased from Sinopharm Chemical Reagent Co. Ltd., China. These reagents were used directly, without further purification, for the synthesis of uric acid precipitates.

Preparation of UA-6 pellet for external calibration

Five grams of UA powder was dissolved in 250 mL of 0.5 mol L^{-1} NaOH solution under constant stirring. Once fully dissolved, 5 g of Solution A was added using a pipette (Pipet-Lite™ XLS+™, Mettler-Toledo, China). The solution was stirred for 10 minutes at room temperature with a magnetic stirrer (H01-1B, Shanghai Meiyingpu Instrument Manufacturing Co. Ltd., China). Subsequently, 100 mL of glacial acetic acid (pre-diluted 10-fold with ultrapure water) was added to induce precipitation. After an additional 5 minutes of stirring, the resulting precipitate was collected by suction filtration and dried at 40 °C to obtain a UA-based material doped with trace elements.

The dried precipitates were finely ground using an agate mortar and pressed into pellets using a manual press (~12 MPa). These pellets were then embedded in epoxy resin mixed with hardener at a 1:3 weight ratio. Surface preparation was completed by sequential polishing with 1000, 3000, 5000, and 7000 grit abrasive papers to yield smooth, analyzable surfaces

Tuning of LA-ICP-MS

Prior to analysis, the laser ablation system was preheated for 30 minutes without performing any ablation to ensure stable performance. Helium (0.6 L min^{-1}) served as the carrier gas within the ablation cell and was mixed with argon (0.8 L min^{-1}) downstream via a T-connector. The NIST SRM 610 silicate glass standard was used throughout the instrumental tuning process to calibrate for sensitivity drift over time and to optimize operational parameters, the latter achieved by maximizing the ^{89}Y signal for high sensitivity. At the same time, the aforementioned system maintained low double-charge yields ($^{42}Ca^{2+}/^{42}Ca^{+} < 0.5\%$) and oxide yields ($^{232}Th^{16}O^{+}/^{232}Th^{+} < 0.5\%$), with a Th/U ratio close to 1 in NIST SRM 610, ensuring minimal polyatomic interferences and good stoichiometric consistency during analysis. Elemental quantitative imaging was performed in line-scan modes using a 90 μm laser beam diameter and an 8 Hz repetition rate. Each element's dwell time was set at 10 ms to capture accurate signal intensities.

Prior to LA-ICP-MS imaging analysis, the washout time of the ablation cell was evaluated by performing 15 single laser shots on the CaOx-1 standard in single-spot mode. The resulting ^{44}Ca signal intensities recorded by ICP-MS were exported in CSV format and plotted against time using Origin 2024 software. The peak widths from all 15 measurements were analyzed and averaged, yielding a mean washout time of 1.42 seconds (Fig.

S4). This enhanced performance, where washout time is defined by a signal descent to the 10% level,[1] is attributed to the modification of the ablation cell, which was filled 70% with plasticine to reduce its internal volume.

External calibration using a dual-standard calibration strategy

A dual-standard calibration strategy was This was performed in Microsoft Excel 2021 using eqn (S1):[2, 3]

$$C_{sam}^{\ i} = C_{sam}^{\ is} \times (C_{std}^{\ i}/C_{std}^{\ is}) \times (I_{sam}^{\ i}/I_{sam}^{\ is})/(I_{std}^{\ i}/I_{std}^{\ is}) \quad \text{(S1)}$$

where $C_{sam}^{\ i}$ is the concentration of the target element in the sample; $C_{sam}^{\ is}$ is the concentration of the internal standard in the sample, which refers to the theoretical carbon mass fraction in UA stones or the theoretical Ca mass fraction in CaOx stones; $C_{std}^{\ i}$ is the concentration of the target element in the calibration standard; $C_{std}^{\ is}$ is the concentration of the internal standard in the calibration standard, which refers to the theoretical carbon mass fraction in UA-6 or the previously reported Ca mass fraction in CaOx-1;[4] $I_{sam}^{\ i}$ is the signal intensity of the target element in the sample; $I_{sam}^{\ is}$ is the signal intensity of the internal standard in the sample; $I_{std}^{\ i}$ is the signal intensity of the target element in the calibration standard; and $I_{std}^{\ is}$ is the signal intensity of the internal standard in the calibration standard.

Evaluation of analytical errors resulted from non-matrix-matched calibration

If a CaOx region is mistakenly identified as UA and calibrated using the UA-6 standard, quantification will be biased. In this context, carbon (C), a major element homogeneously distributed in both CaOx and UA, was used as the internal standard for signal correction. Based on eqn (S1), the impact of misidentification can be deduced and expressed as eqn (S2), which compares the erroneous result to the true value.

$$\frac{C_{samincorrect}^{i}}{C_{samtrue}^{i}} = \frac{C_{UA}^{i}/C_{UA}^{C}}{C_{CaOx}^{i}/C_{CaOx}^{C}} \times \frac{I_{CaOx}^{i}/I_{CaOx}^{C}}{I_{UA}^{i}/I_{UA}^{C}} = \frac{RSC_{CaOx}^{i}}{RSC_{UA}^{i}} \times \frac{RSC_{UA}^{C}}{RSC_{CaOx}^{C}} \quad \text{(S2)}$$

where $C_{samincorrect}^{i}$ is the concentration of the target element in the sample when UA-6 is erroneously used to calibrate the CaOx textures; $C_{samtrue}^{i}$ is the concentration of the target element in the sample under matrix-matched calibration. C_{UA}^{i} is the concentration of the target element in UA-6; C_{UA}^{C} is the mass fraction of the internal standard ^{13}C in UA-6. C_{CaOx}^{i} is the concentration of the target element in CaOx-1; C_{CaOx}^{C} is the mass fraction of the internal standard ^{13}C in CaOx-1. I_{CaOx}^{i} is the signal intensity of the target element in CaOx-1; I_{CaOx}^{C} is the signal intensity of the internal standard ^{13}C in CaOx-1. I_{UA}^{i} is the signal intensity of the target element in UA-6; I_{UA}^{C} is the signal intensity of the internal standard ^{13}C in CaOx-1.

To account for matrix effects, a correction factor was introduced and calculated using eqn (S3).

$$k_i = \frac{RSC_{UA}^{i}}{RSC_{CaOx}^{i}} \quad \text{(S3)}$$

where k_i represents the matrix effect correction factor; RSC_{UA}^{i} denotes the *RSC* of the target element in UA-6; RSC_{CaOx}^{i} is the *RSC* of the target element in CaOx-1. Here, the *RSC* values of carbon in CaOx-1 and UA-6 were calculated, the results were as follows: RSC_{CaOx}^{C} = 5.91×10^5 cps (μg g^{-1})$^{-1}$ and RSC_{UA}^{C} = 9.00×10^5 cps (μg g^{-1})$^{-1}$. Based on these values, the correction factor of C, k_C, can be calculated to be 1.52.

Substituting this into eqn (S2), the expression can be simplified to eqn (S4) as follows:

$$\frac{C_{samincorrect}^{i}}{C_{samtrue}^{i}} = \frac{RSC_{CaOx}^{i}}{RSC_{UA}^{i}} \times 1.52 \quad \text{(S4)}$$

If the matrix composition of complex-textured samples is misidentified, leading to the inappropriate selection of calibration standards, significant analytical errors may be introduced. These errors primarily arise from the following:

(1) Matrix effect-induced discrepancies in the *RSC*s of trace elements. Matrix effect correction factors (*k*) were calculated using eqn (S2) based on the *RSC* values presented in Fig. 2 in the main text, yielding the following results: 9.74 for Mg, 7.97 for Cr, 0.856 for Mn, 7.50 for Co, 5.94 for Cu, 0.537 for Zn and 8.42 for Sr. Considering the difference in carbon *RSC*s between CaOx and UA, the ratio $\frac{C_{samincorrect}^{i}}{C_{samtrue}^{i}}$ can be calculated to

be 0.16 for Mg, 0.19 for Cr, 1.77 for Mn, 0.20 for Co, 0.26 for Cu, 2.83 for Zn and 0.18 for Sr. Based on these ratios, the corresponding relative errors in quantification were estimated using eqn (S5).

$$E_r = \frac{C^{\,i}_{samincorrect} - C^{\,i}_{samtrue}}{C^{\,i}_{samtrue}} \times 100\% = \left(\frac{C^{\,i}_{samincorrect}}{C^{\,i}_{samtrue}} - 1\right) \times 100\% \quad \text{(S5)}$$

According to eqn (S4), the relative errors were calculated to be -84% for Mg, -81% for Cr, 77% for Mn, -80% for Co, -74% for Cu, 183% for Zn, and -82% for Sr, indicating that substantial deviations may occur if the matrix composition of dual-matrix urinary stones is misidentified, and inappropriate calibration standards are applied.

(2) Severe computational errors due to improper internal standard selection. For instance, misidentifying UA regions as CaOx could result in the erroneous use of ^{44}Ca (appropriate for CaOx matrices) instead of ^{13}C (optimal for UA matrices) as the internal standard. Given the inherently low Ca content in UA stones, ranging from 0.01% to 1.51% in pure UA stones (as determined by EPMA in our previous study) and 0.02% to 1.57% in UA textures in this work, such a misselection would introduce unpredictable errors during internal standard calibration. Thus, matrix misjudgment can propagate compounded inaccuracies through inappropriate internal standard selection.

Moreover, for CaOx matrices, Ca is often a suitable internal standard. As a primary matrix element of CaOx, Ca shares similar ionization energy and chemical properties with certain trace metals such as Sr, enabling more

accurate representation of matrix-related ionization behaviors and consequently mitigating matrix effect-induced biases in the analytical results. In contrast, carbon (^{13}C), commonly used as an internal standard in organic matrices,[5, 6] may be less suitable in predominantly inorganic matrices like CaOx. Its application in complex inorganic matrices could potentially introduce additional uncertainties due to its high first ionization potential (11.3 eV).[6, 7]

Detection of matrix composition using SEM-EDS and EPMA

Significant color differences and complex textural characteristics were observed on the surface of the real sample, as shown in Fig. S3a. These features were classified into two distinct regions: black regions (I and II) and gray regions (III and IV). The color variations likely arise from differences in matrix composition or microstructural changes due to uneven elemental distribution. To better understand the matrix composition of each region, a systematic study was conducted using SEM-EDS, EPMA, and LA-ICP-MS techniques.

Initially, semi-quantitative SEM-EDS imaging was used to identify the matrix composition of UA and CaOx. As shown in Fig. S3b, regions with higher mass fractions of N were consistent with the black regions in Fig. S3a, indicating these regions correspond to the UA matrix. Similarly, regions with a higher mass fraction of Ca in Fig. S3c were consistent with the gray regions in Fig. S3a, confirming that the gray regions correspond to CaOx.

Further SEM-EDS analysis was performed in each region. The first (I) and second (II) analyses of the black regions detected C (~0.277 keV), N (~0.393 keV), and O (~0.525 keV) (Figs. S3d and S3f). The third (III) and fourth (IV) analyses of the gray regions revealed C (~0.277 keV), O (~0.523 keV), and Ca (~3.69 keV for Kα spectrum, ~4.09 keV for Kβ spectrum), further confirming that the black and gray regions represent UA

and CaOx, respectively. This also demonstrates that the urinary stone is a dual-matrix sample.

To further confirm these findings, semi-quantitative EPMA analyses were conducted in both the black and gray regions, with 40 spot analyses in the black regions and 30 in the gray regions. The results, shown in Table S3, reveal that the black regions contain a low mass fraction of Ca (0.15 ± 0.26 wt.%), but high mass fractions of N (26.23 ± 1.91 wt.%), confirming the matrix composition of UA. In contrast, the gray regions contained a high mass fraction of Ca (26.98 ± 1.04 wt.%) and a very low mass fraction of N (0.79 ± 0.69 wt.%), indicating their composition of CaOx. Therefore, the urinary stone can be concluded to be composed of both UA and CaOx. It should be noted that these data just serve as semi-quantitative or

Reference

1. E. L. Gurevich and R. Hergenroeder, *J. Anal. At. Spectrom.*, 2007, **22**, 1043-1050.
2. Y. Zhang, S. Y. You, F. W. Tan, J. F. Shao, J. Z. Zhou, T. F. Zheng, W. X. Yi, P. Xia, L. L. Jin, H. T. Li, R. X. Wang, H. R. Wen, Y. Q. Ke and Y. J. Sun, *Geostand. Geoanal. Res.*, 2023, **47**, 773-792.
3. H. P. Longerich, S. E. Jackson and D. Günther, *J. Anal. At. Spectrom.*, 1996, **11**, 899-904.
4. H. Deng, H. Xu, J. Zhou, D. Tang, W. Yang, M. Hu, Y. Zhang and Y. Ke, *Anal. Bioanal. Chem.*, 2023, **415**, 1751-1764.
5. K. Chacon-Madrid and M. A. Z. Arruda, *J. Anal. At. Spectrom.*, 2018, **33**, 1720-1728.
6. D. A. Frick and D. Günther, *J. Anal. At. Spectrom.*, 2012, **27**, 1294-1303.
7. M. Resano, E. García-Ruiz and F. Vanhaecke, *Spectrochim. Acta Part B*, 2005, **60**, 1472-1481.

Table S1 Operating parameters for LA-ICP-MS analysis

LA	
Laser ablation system	ArF excimer laser
Wavelength, nm	193
Beam diameter, μm	90
Energy density, J cm^{-2}	8
Repetition rate, Hz	8
Carrier gas (He) flow rate, L min^{-1}	0.6
Scan speed, μm s^{-1}	20
ICP-MS	Agilent 7900
RF power, W	1550
Sampling depth, mm	10
Plasma gas (Ar) flow rate, L min^{-1}	15
Auxiliary gas (Ar) flow rate, L min^{-1}	0.8
Dwell time, ms	10
Monitored isotopes	^{13}C, ^{25}Mg, ^{44}Ca, ^{53}Cr, ^{55}Mn, ^{59}Co, ^{63}Cu, ^{66}Zn, ^{88}Sr

Table S2 Identification of matrix composition using a moving-window *t*-test approach

Data No.	1	2	3	4	5	6	7	8	9	10	11	12	13	14	15	…	*n*	*t* value	Meaning
1st test	s_1												s_2					t_1	If t_1 exceeds the critical $t_{critical}$, it indicates a matrix alteration, in which case the 13th data point should be calculated using a new matrix-matched external standard. Otherwise, no matrix change is detected, and the previous external standard may continue to be applied.
2nd test		s_1												s_2				t_2	If t_2 exceeds the critical $t_{critical}$, it indicates a matrix alteration, in which case the 14th data point should be calculated using a new matrix-matched external standard. Otherwise, no matrix change is detected, and the previous external standard may continue to be applied.
3rd test			s_1												s_2			t_3	If t_3 exceeds the critical $t_{critical}$, it indicates a matrix alteration, in which case the 15th data point should be calculated using a new matrix-matched external standard. Otherwise, no matrix change is detected, and the previous external standard may continue to be applied.
….				s_1												s_2		…	….
***n*th test**					s_1												s_2	t_n	If t_n exceeds the critical $t_{critical}$, it indicates a matrix alteration, in which case the n^{th} data point should be calculated using a new matrix-matched external standard. Otherwise, no matrix change is detected, and the previous external standard may continue to be applied.

Table S3 The mass fraction (Mean ± 1*s*, wt.%) of Ca, N, O, and K in the black (*n*=40) and gray (*n*=30) regions in the real urinary stone determined by EPMA

Region	Ca	N	O	K
Black	0.15 ± 0.26	26.23 ± 1.91	29.32 ± 1.34	0.08 ± 0.04
Gray	26.98 ± 1.04	0.79 ± 0.69	47.78 ± 1.26	<DL

<DL, lower than detection limit

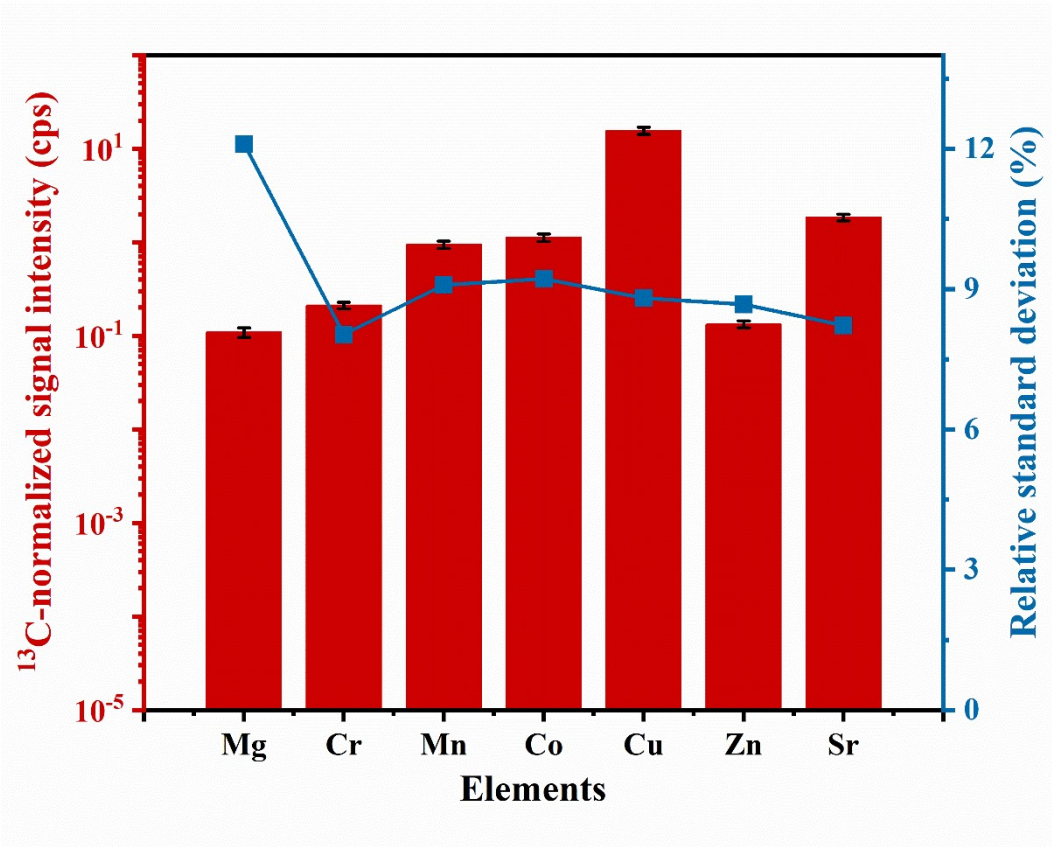

Fig. S1 Homogeneity assessment of trace elements in the UA-6 pellet. The relative standard deviation (RSD) of ^{13}C-normalized signal intensities (1 *s*, *n* = 28 repeated measurements) for Mg, Cr, Mn, Co, Cu, Zn, and Sr is primarily below 10%, demonstrating a generally homogeneous distribution

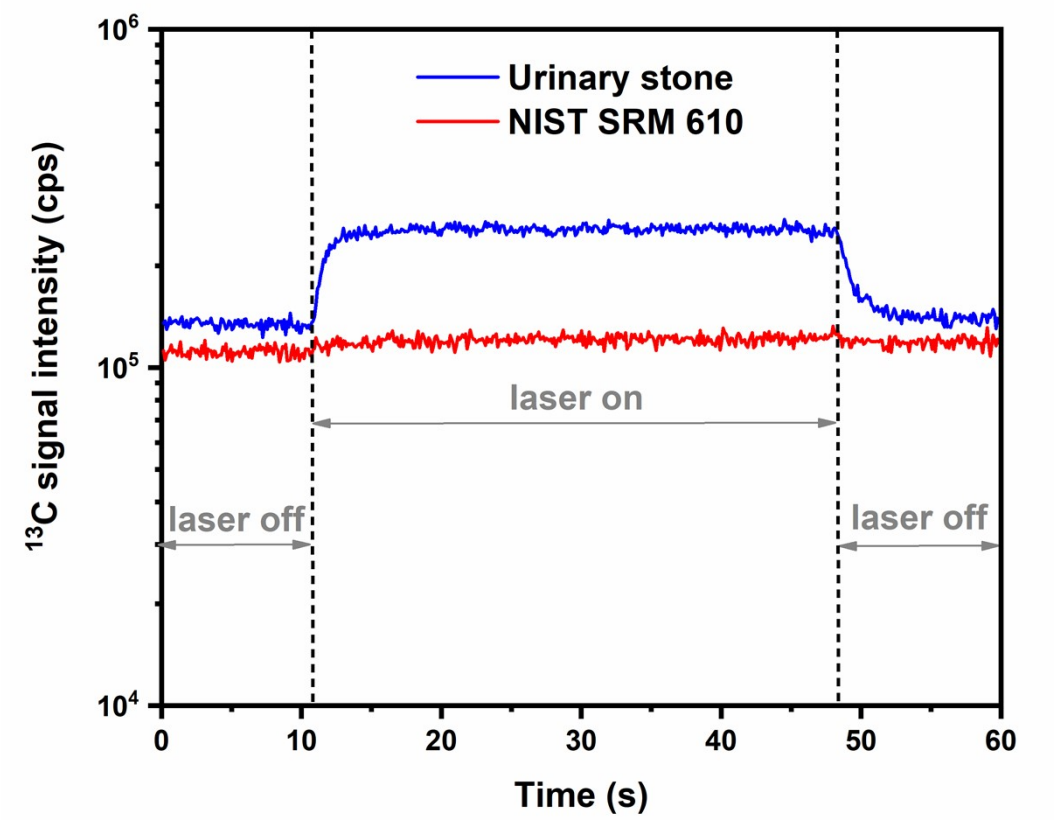

Fig. S2 ^{13}C signal profiles in NIST SRM 610 and urinary stone. The ^{13}C signal intensity in NIST SRM 610 remains stable from laser-on to laser-off (gas blank) conditions, indicating no detectable carbon contamination on the sample surface after polishing with SiC abrasive papers

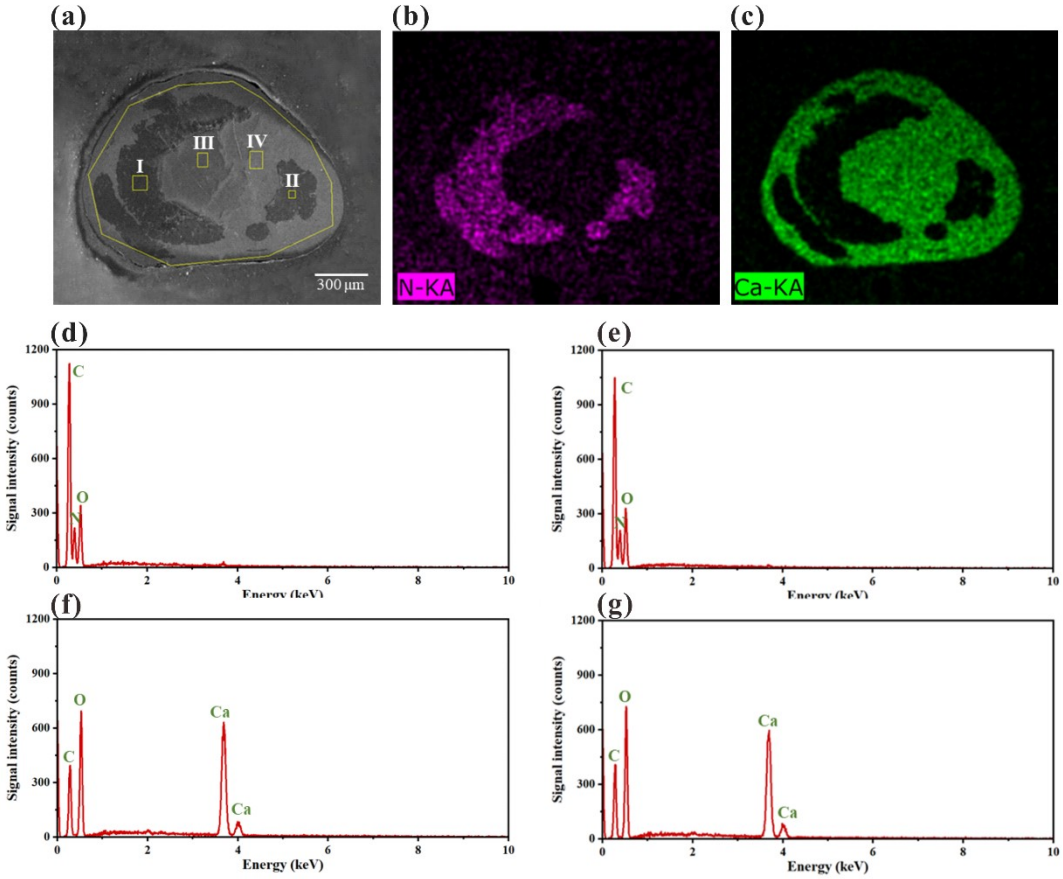

Fig. S3 BSE image of the real urinary stone surface (a), along with SEM-EDS images of nitrogen (b) and calcium (c) in the urinary stone, revealing the distribution of UA and CaOx within the stone. The black regions (I) and (II) in the BSE image were identified as UA, as shown in the EDS spectra (d) and (e), respectively. The gray regions (III) and (IV) in the BSE image were identified as CaOx, as illustrated in the EDS spectra (f) and (g), respectively

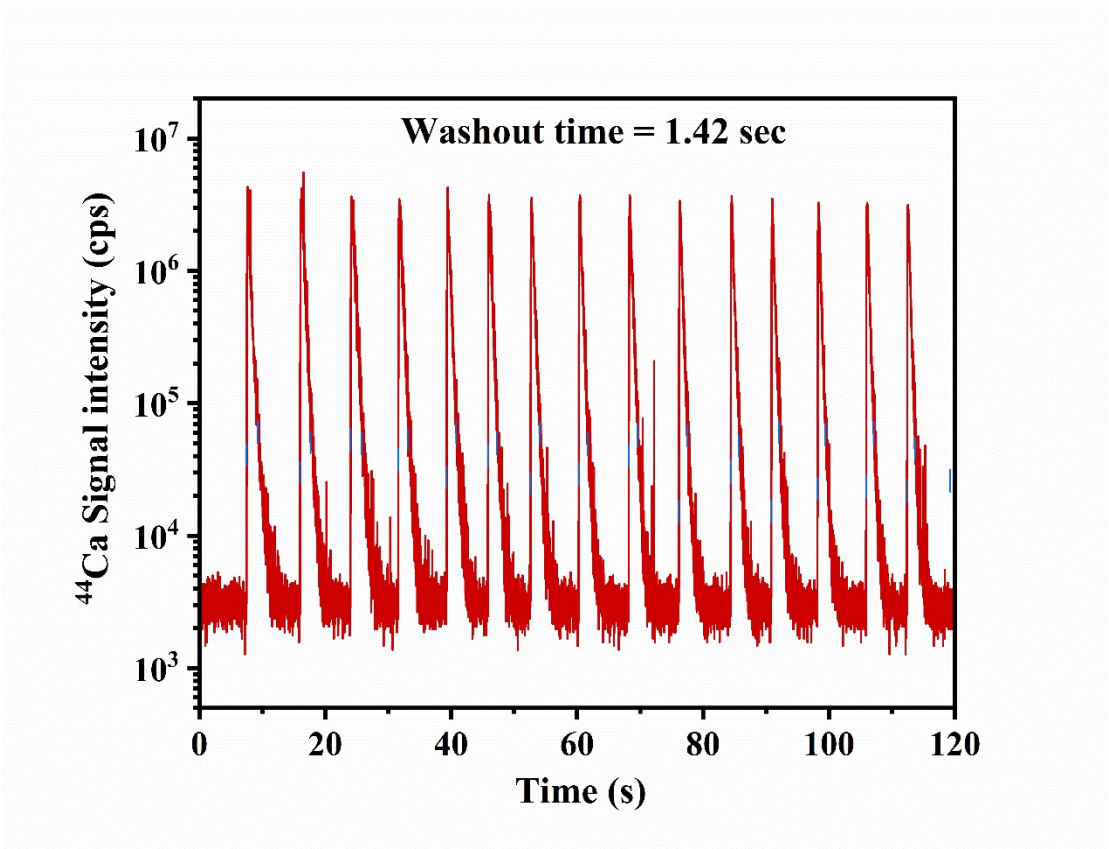

Fig. S4 The ^{44}Ca signal profile from 15 LA-ICP-MS single spot analyses shows a washout time of 1.42 sec

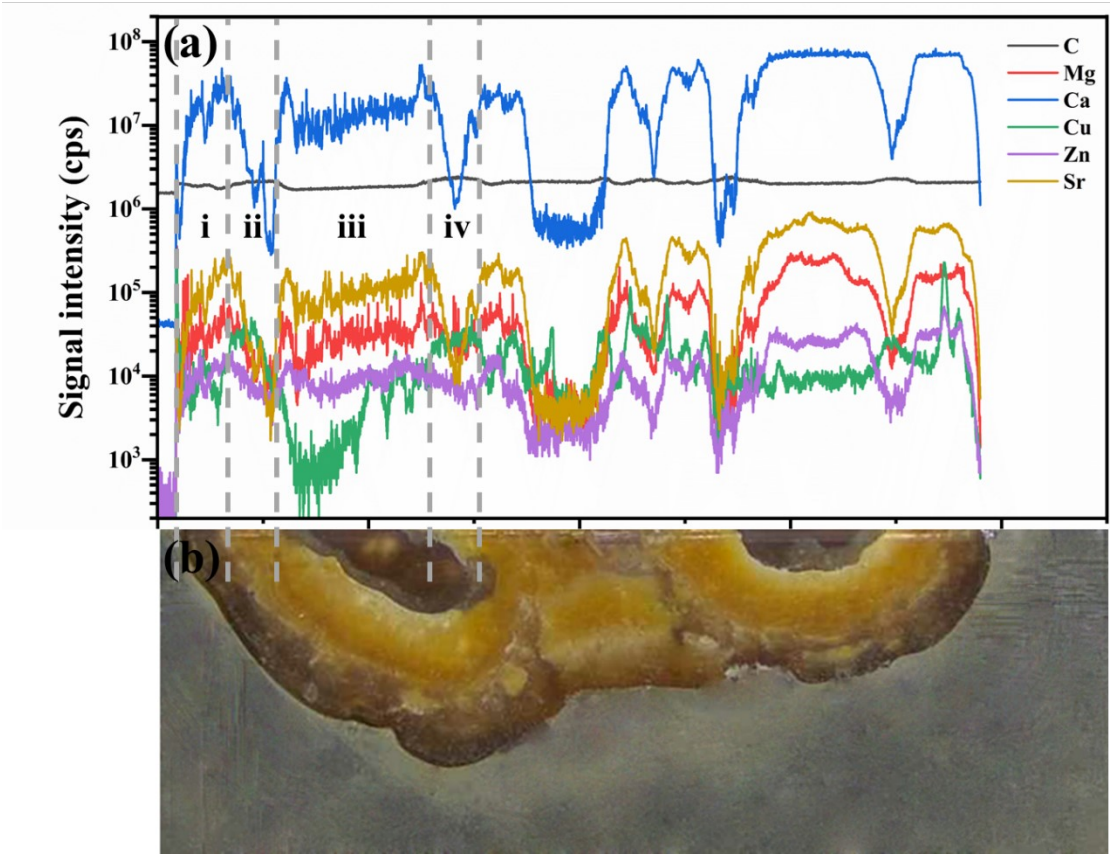

Fig. S5 LA-ICP-MS line scan signal profiles (a) corresponding to the line scan track on the second urinary stone (b) shows a strong negative correlation between the Ca and C signals, especially for intervals i, ii, iii, and iv